

| | |
|--------------|--|
| Title | Formation of NiAl intermetallic compound from powder mixture of nickel and aluminum by laser irradiation |
| Author(s) | Matsumoto, Ryo; Komaki, Shota; Homi, Ryohei et al. |
| Citation | Materials Transactions. 2021, 62(4), p. 512-518 |
| Version Type | VoR |
| URL | https://hdl.handle.net/11094/94007 |
| rights | |
| Note | |

Osaka University Knowledge Archive : OUKA

<https://ir.library.osaka-u.ac.jp/>

Osaka University

Formation of NiAl Intermetallic Compound from Powder Mixture of Nickel and Aluminum by Laser Irradiation

Ryo Matsumoto*, Shota Komaki, Ryohei Homi and Hiroshi Utsunomiya

Division of Materials and Manufacturing Science, Osaka University, Suita 565-0871, Japan

NiAl intermetallic compound was formed by laser irradiation on powder mixture of nickel and aluminum. In laser irradiation with an average energy density of 150 J/mm² using a continuous wave 50 W Nd:YAG laser, Ni–49 at% Al powder mixture was immediately heated up to a temperature above 1680 K by reaction heat on the interface between nickel and aluminum powders. As the result, the powder mixture was ignited with maximum bulk volume of approximately 1.0×10^4 mm³, and the powder mixture was partly melted. After solidification of the melted part by natural cooling, the formation of NiAl intermetallic compound was confirmed from the results of microscopic observations, hardness measurement, EDX and XRD analyses. [[doi:10.2320/matertrans.MT-M2020319](https://doi.org/10.2320/matertrans.MT-M2020319)]

(Received October 12, 2020; Accepted January 12, 2021; Published February 15, 2021)

Keywords: laser irradiation, powder mixture, intermetallic compound, reaction heat, nickel, aluminum

1. Introduction

Nickel aluminide (Ni–Al) intermetallic compounds are attractive material as lightweight and heat-resistant structural materials due to high specific strength, high melting point and high-temperature oxidation resistance. L1₂ type Ni₃Al (γ') and B2 type NiAl (β) intermetallic compounds are widely considered for industrial applications.¹⁾ Owing to the highest melting point (1911 K) among Ni–Al intermetallic compounds as well as high thermal conductivity and high oxidation resistance, NiAl intermetallic compound is practically used for coating material for engines and turbine parts for aerospace, automotive and power plants.²⁾

Mass production of the intermetallic compounds generally starts from melting process. The crystal structure of the intermetallic compounds can be stable after solidification from a liquid phase. Therefore the metals must be heated to very high temperature because of high melting point of the intermetallic compounds. In order to obtain ordered compound, they must be kept to very high temperature at least several hours. Reaction synthesis processing is known as one of the formation method for the intermetallic compounds.³⁾ The processing was confirmed to be effective for the formation of the Ni–Al intermetallic compound.⁴⁾ The formation of the Ni–Al intermetallic compound in the reaction synthesis was reviewed as follows.⁵⁾ Diffusion of aluminum atoms into nickel occurs on the interface of nickel and aluminum by heating them above the melting point of aluminum (933 K). The reaction heat is generated on the interface between nickel and aluminum during formation of the compound by diffusion of aluminum. Then the reaction synthesis occurs in a chain between nickel and aluminum due to high enthalpy change. In powder metallurgy process of powder mixture of nickel and aluminum, the influences of heating rate⁶⁾ and press pressure⁷⁾ on the formation of the Ni–Al intermetallic compound were investigated. Reaction synthesis processing was applied for formation of Ni–Al intermetallic foams.⁸⁾ The microstructure of the Ni–Al

intermetallic compound formed by powder metallurgy process with reaction synthesis was also reported.^{9,10)} On the other hand, reaction synthesis processing for formation of Ti–Al intermetallic compounds from powder mixture compact of titanium and aluminum was reported.¹¹⁾

Owing to local heating and rapid cooling of metal, laser processing is also applied to the formation of Ni–Al intermetallic compounds. Ni–Al intermetallic compounds were reported to be formed from mixture compacts of nickel and aluminum by laser sintering using a 2 kW CO₂ laser.¹²⁾ Ni–Al intermetallic compound layers were also reported to be formed from powder mixture of nickel and aluminum on the steel substrate by laser cladding using a continuous wave 10 kW CO₂ laser.¹³⁾ However, the further investigations on the formation conditions and mechanism are required for the industrial uses. In these laser processes, the reaction heat was generated on the interface between nickel and aluminum. Due to the reaction heat, Ni–Al intermetallic compounds may be formed under a low laser energy. Since it is known that the composition for stable ordered crystal structure of NiAl at room temperature is relatively wide as Ni–(46–54) at% Al,¹⁴⁾ NiAl intermetallic compound with practically acceptable composition may be formed by laser irradiation on the powder mixture. In addition, the laser irradiation on the powder mixture has a potential to fabricate the bulk body of the intermetallic compounds with different compositions at each part by controlling the mixture ratio of the powder mixture if the reaction heat can be controlled accurately.

In this study, NiAl intermetallic compound is formed by laser irradiation on powder mixtures of nickel and aluminum using a continuous wave 50 W Nd:YAG laser. The powder mixture is melted and solidified by the laser irradiation with an average energy density of 150 J/mm². The formed phases in the laser-irradiated part are identified by microscopic observations, hardness measurement, energy dispersive x-ray spectrometry (EDX) and x-ray diffraction (XRD) pattern analyses. The formation mechanism is discussed from viewpoint of reaction heat.

*Corresponding author, E-mail: ryo@mat.eng.osaka-u.ac.jp

Table 1 Characteristics of nickel and aluminum powders used in this study.

| Powder | Purity / mass % | Particle diameter / μm | Bulk density / $\text{g} \cdot \text{cm}^{-3}$ |
|----------|--------------------|---|--|
| Nickel | > 99.9 | 10–20 | 4.36 |
| Aluminum | > 99.8 | < 30 | 0.62 |

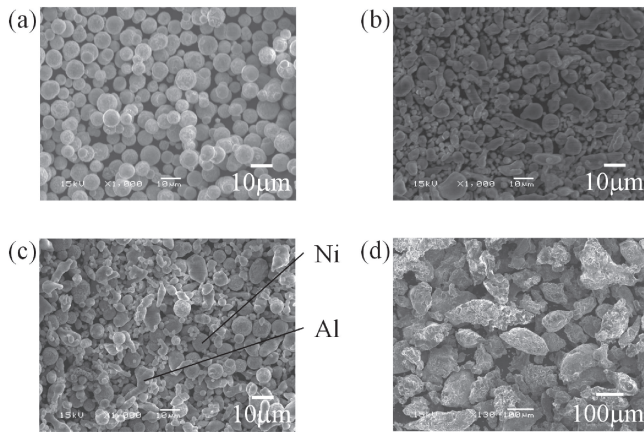


Fig. 1 Scanning electron microscope (SEM) photographs of powders used in this study. (a) nickel, (b) aluminum, (c) Ni-49 at% Al mixture, (d) NiAl intermetallic compound.

2. Experimental Procedures

2.1 Nickel and aluminum powders

Commercially pure nickel (>99.9 mass%) and aluminum (>99.8 mass%) powders were used. The powders were commercial ones (Nilaco Corporation). The characteristics of the powders are shown in Table 1. The powders were presumed to be manufactured by the atomization method because the powder shapes of the nickel and aluminum were spherical and teardrop shapes shown as Fig. 1(a), (b), respectively.

The powders were mixed with following weight ratios by dry powder milling for 30 minutes using yttria-stabilized zirconia (YSZ) balls with a diameter of 10 mm. From consideration of Ni–Al binary phase diagram,¹⁵⁾ Ni-49 at% Al (Ni-31 mass% Al) powder mixture was prepared for formation of NiAl intermetallic compound, while Ni-32 at% Al (Ni-18 mass% Al) powder mixture was prepared for comparison. Dual phase of Ni_5Al_3 and Ni_3Al intermetallic compounds is formed from Ni-32 at% Al in the equilibrium condition. The scanning electron microscope (SEM) photograph of the Ni-49 at% Al powder mixture is shown in Fig. 1(c).

To examine occurrence of the ignition, NiAl intermetallic compound powder was also irradiated with laser. The powder was prepared by crushing manually the NiAl intermetallic compound using a mortar and pestle. Dry powder milling of the crushed powder was performed under the same conditions for the powder mixtures. The NiAl intermetallic compound was prepared by combusting and solidifying the Ni-49 at% Al powder mixture by laser irradiation. The SEM

photograph of the prepared powder of the NiAl intermetallic compound was shown in Fig. 1(d). The shape of the prepared powder was horn shape, and the particle size of the prepared powder was less than 200 μm in diameter.

2.2 Laser irradiation conditions

Figure 2(a), (b) shows the photograph and schematic illustration of the experimental apparatus for laser irradiation. The apparatus mainly consisted of a laser oscillator, a container, a chamber, a manual z-axis stage and a computer. The laser oscillation and scanning on the x-y plane were controlled by the computer, while the vertical position (z) of the container was manually adjusted by the z-axis stage. A continuous wave 50 W Nd:YAG laser (Miyachi Corporation: ML-7062A, average power: 30 W) with Q-switch mode was used for laser irradiation. The peak output (P_p), pulse interval (w) and pulse frequency (f) in Q-switch mode were set to be 25 kW, 200 ns and 6 kHz, respectively. The laser spot diameter was set to be $d_s = 0.2 \text{ mm}$ by adjusting the defocus amount (distance from laser focus). The laser beam was scanned with speed of $v_s = 1 \text{ mm/s}$ in the x and y directions. The average energy density of the laser beam was set to $E_{\text{avg}} = P_p \cdot w \cdot f / (d_s \cdot v_s) = 150 \text{ J/mm}^2$. These laser irradiation conditions (P_p , w , f , d_s , v_s) were determined from laser irradiation conditions for aluminum powder in our previous research work.¹⁶⁾

The laser scanning on the x-y plane was controlled by inclination angles of a galvanometer mirror in the laser oscillator. As shown in Fig. 2(c), the laser was scanned in an area of 10 mm in the x direction and 10 mm in the y direction on the surface of the powder bed. The laser was scanned on the periphery edge of the area, then it was scanned in the area in the y direction with a hatching pitch of 0.2 mm in the x direction from the left edge of the area. The overlap of the laser scanned areas in the x direction was none.

The powder was supplied with a thickness of 5 mm in the cylindrical ceramic container with a diameter of 20 mm and a thickness of 5 mm, then the top surface of the supplied powder was manually flattened by using a wiper. The surface roughness and the relative density of the powder beds were approximately 110 μm and 0.43, respectively. The powder started to be irradiated with laser after replacing the atmosphere in the chamber with argon (pressure: 0.1 MPa).

2.3 Identification methods for intermetallic compounds

Formed phases in the laser-irradiated part were identified by microscopic observations, hardness measurement, EDX and XRD analyses. The x-y surface and x-z cross-section of the laser-irradiated part were observed by an optical microscope (OM) and a scanning electron microscope (SEM). Vickers hardness in the x-z cross-section of the laser-irradiated part was measured with indentation load of 2 N and loading duration of 20 s. The element map of the formed phases was measured at 0–1.0 mm in the z direction of the x-z cross-section of the laser-irradiated or ignited part by EDX analysis. The XRD pattern was measured at the center area of 2 mm in the x direction and 10 mm in the y direction in the x-y surface of the laser-irradiated or ignited part by x-ray diffractometer with $\text{CuK}\alpha$ line under diffraction angles of 30–120°.

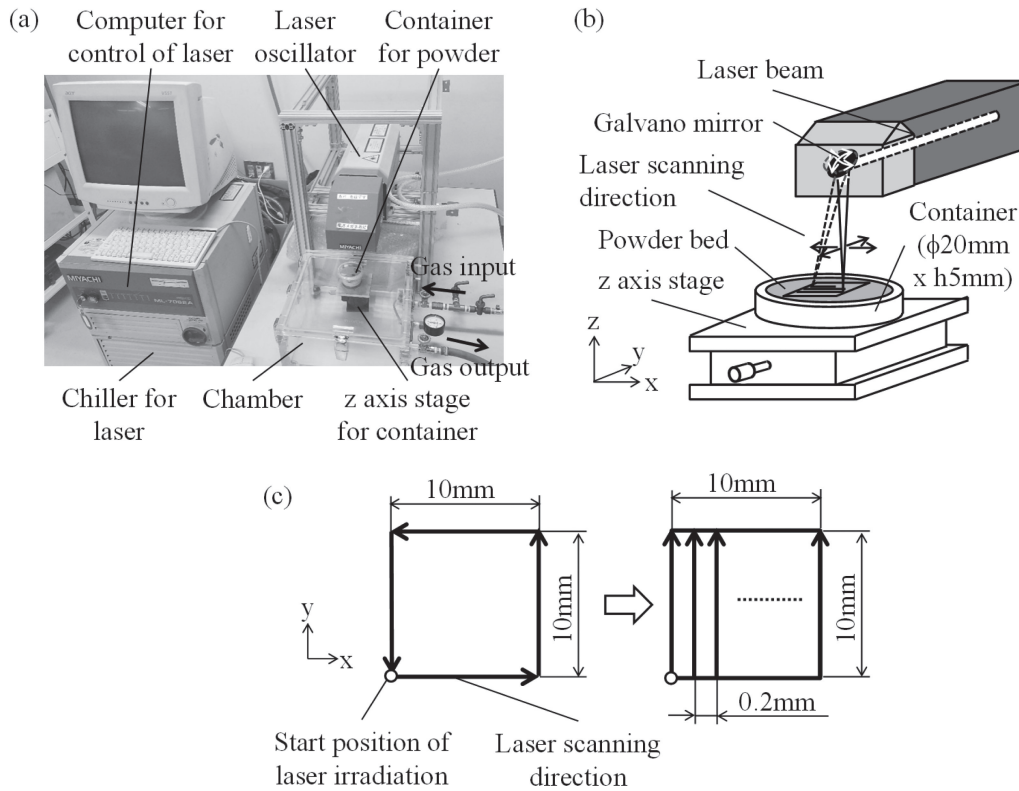


Fig. 2 Experimental apparatus for laser irradiation and schematic illustrations. (a) photograph of apparatus for laser irradiation, (b) schematic illustration of laser irradiation part, (c) laser scanning passes.

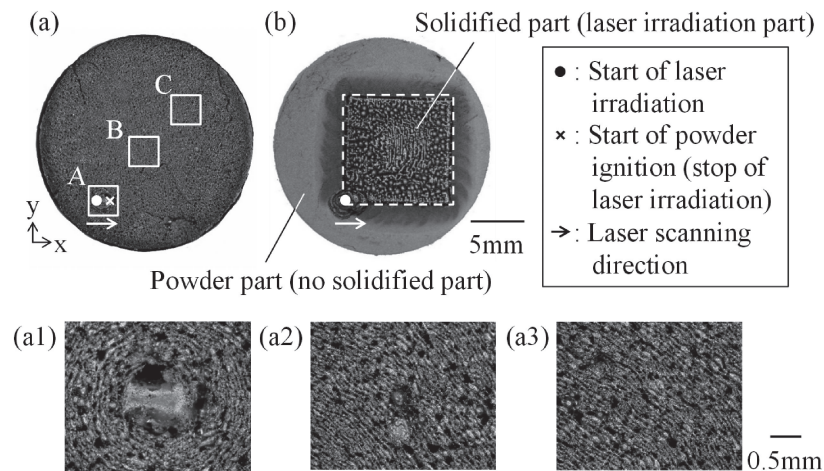


Fig. 3 Photographs of x-y surface of powder mixtures after laser irradiation. (a) Ni-49 at% Al (ignition), (a1) A part, (a2) B part (no laser irradiation part), (a3) C part (no laser irradiation part), (b) Ni-32 at% Al (no ignition).

3. Experimental Results

3.1 Observation of laser-irradiated part

Figure 3 shows the OM photographs of the x-y surface of the powder mixtures after laser irradiation. In laser irradiation on the Ni-49 at% Al powder mixture, the laser-irradiated part of the powder mixture was ignited with intense light immediately after laser irradiation (irradiation duration: 0.1 s, scan distance: 0.1 mm in the x direction), and the ignition was spread throughout the powder mixture in the container. The laser irradiation was stopped immediately after initiation of the ignition in the experiment, however the ignition

continued for a certain duration. In the A part (Fig. 3(a1)) where ignition of the powder mixture was initiated, a concentric pattern centered on the laser-irradiated part was observed. In the B (Fig. 3(a2)) and C (Fig. 3(a3)) parts where ignition of the powder mixture occurred, the concentric pattern centered on the A part was observed. This is because thermal shrinkage of the powder mixture occurred due to ignition of the powder mixture. On the other hand, ignition of the Ni-32 at% Al powder mixture did not occur in laser irradiation on the powder mixture, and the powder mixture was melted and solidified only at the laser-irradiated part as shown in Fig. 3(b).

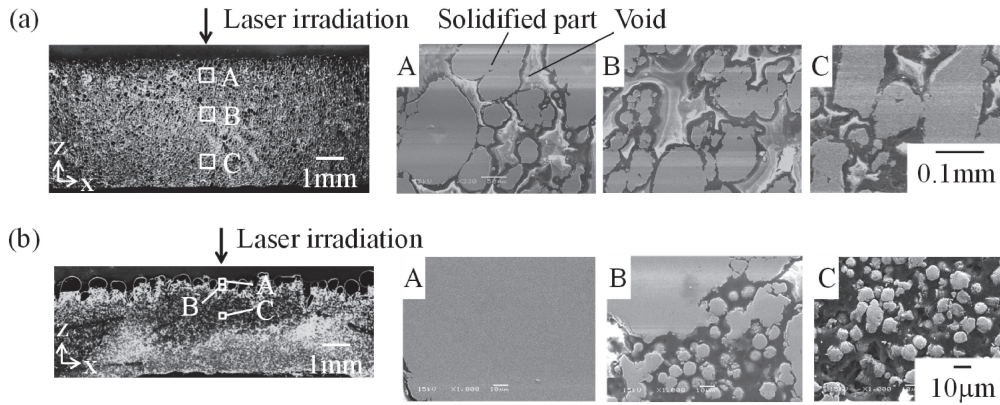


Fig. 4 Photographs of x-z cross-section of powder mixtures after laser irradiation. (a) Ni-49at% Al (ignition), (b) Ni-32at% Al (no ignition).

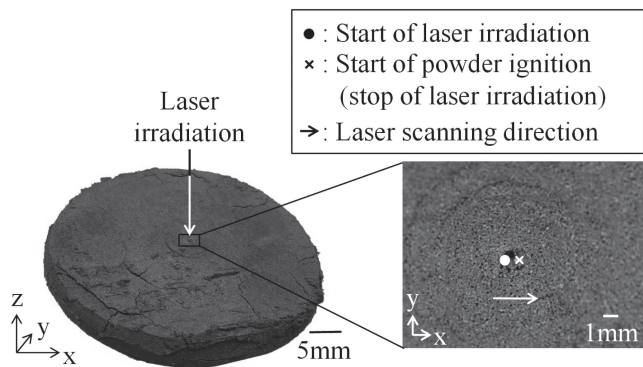


Fig. 5 Photograph of Ni-49at% Al powder mixture solidified after ignition by laser irradiation.

Figure 4 shows the SEM photographs of the x-z cross-section of the laser-irradiated part of the powder mixtures. In laser irradiation on Ni-49at% Al powder mixture, melting and solidification of the powder mixture over the particle size of nickel and aluminum powder was observed from the surface to the bottom of the powder bed (thickness: 5 mm), however some voids were also observed. The mean bulk density and relative density of the powder mixture in the ignition part were 2.30 g/cm^3 and 0.42 (on assumption of NiAl), respectively. The relative density in the ignition part was almost the same with the initial powder bed. On the other hand, melting and solidification of the Ni-32at% Al powder mixture were observed at 0–1 mm in the -z direction from the laser-irradiated surface as shown in Fig. 4(b), while the powder mixture was not melted and solidified at 1–5 mm in the -z direction from the laser-irradiated surface.

To examine the maximum ignition volume of the Ni-49at% Al powder mixture by laser irradiation, the powder mixture was filled in a rectangular container with 90 mm in the x direction \times 90 mm in the y direction \times 10 mm in the z direction for a thickness (z direction) of 5 mm (supplied volume: $4.1 \times 10^4 \text{ mm}^3$). The powder mixture was irradiated with laser at the center of the x-y surface of the rectangular container. Ignition of the powder mixture occurred immediately after laser irradiation, and the powder mixture was melted and solidified as shown in Fig. 5. The bulk volume of the solidified powder mixture was calculated to be

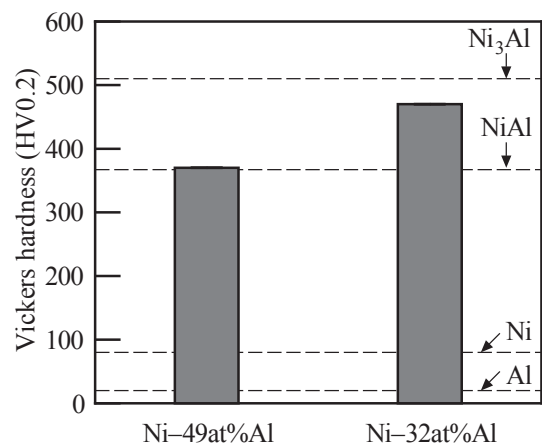


Fig. 6 Average Vickers hardness of x-z cross-section of powder mixtures solidified by laser irradiation.

approximately $1.0 \times 10^4 \text{ mm}^3$ by Archimedes' principle. Thus the maximum bulk volume of the ignited powder mixture was approximately $1.0 \times 10^4 \text{ mm}^3$ under the laser irradiation conditions in this study.

Ignition of unmixed powder of nickel or aluminum did not occur in laser irradiation on the powder with $E_{avg} = 150 \text{ J/mm}^2$, and the unmixed powder was melted and solidified at 0–0.5 mm in the -z direction from the laser-irradiated surface.

3.2 Vickers hardness

Figure 6 shows the Vickers hardness of the solidified powder mixtures in the x-z cross-section of the laser-irradiated part. The powder mixtures were solidified in the laser-irradiated part as described in Section 3.1. The hardness of the solidified Ni-49at% Al powder mixture (A part in Fig. 4(a)) was almost the same with that of NiAl (about 367 HV¹⁷), while the hardness of the solidified Ni-32at% Al powder mixture (A and B parts in Fig. 4(b)) was almost the same with that of Ni₃Al (about 510 HV¹⁸). Precipitation hardening occurred due to the solid solution of nickel and aluminum in each crystal lattice, so that the hardness of the solidified powder mixtures dramatically increased above nickel (80 HV¹⁹) and aluminum (20 HV²⁰).

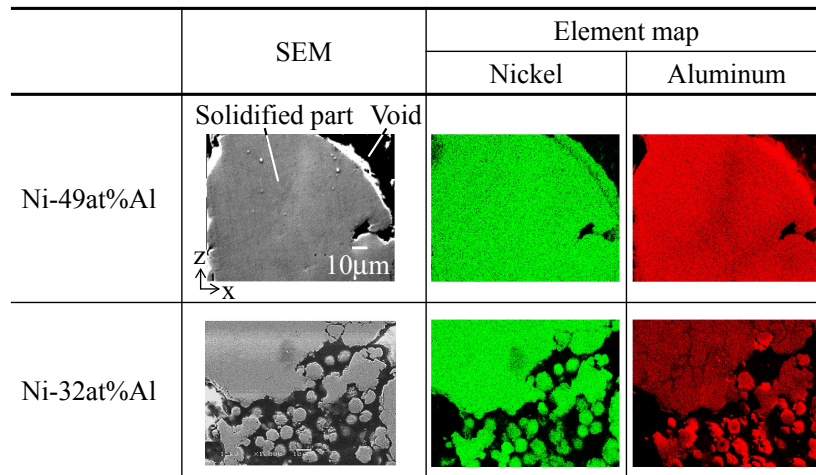


Fig. 7 Element map of x-z cross-section of powder mixtures solidified by laser irradiation.

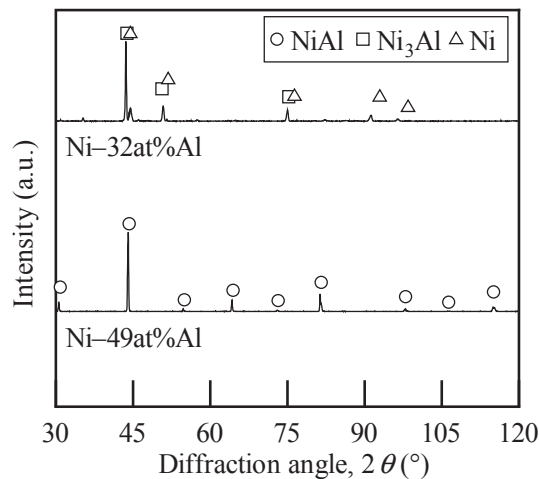


Fig. 8 X-ray diffraction pattern from x-y surface of powder mixtures solidified by laser irradiation.

3.3 EDX and XRD analyses

Figure 7 shows the element map of the x-z cross-section of the powder mixtures solidified by laser irradiation. It seems that the Ni-49at% Al powder mixture was wholly melted and diffused, while the Ni-32at% Al powder mixture was partly melted, and powders and voids were also detected. Therefore the Ni-49at% Al powder mixture was heated sufficiently for diffusion of nickel and aluminum, while the Ni-32at% Al powder mixture was not heated sufficiently for diffusion.

Figure 8 shows the x-ray diffraction pattern of the x-y surface from the powder mixtures solidified by laser irradiation. The peak intensities of NiAl were detected in the solidified Ni-49at% Al powder mixture, while those of other Ni-Al intermetallic compounds, nickel and aluminum were not detected. Although formations of Ni_3Al_3 and Ni_3Al were predicted from Ni-Al binary phase diagram¹⁵⁾ in laser irradiation on the Ni-32at% Al powder mixture, the peak intensities of Ni_3Al and nickel were detected. This result agrees with the results of the hardness test (solidified Ni-32at% Al powder mixture: 470 HV0.2, Ni_3Al : 510 HV0.2, Fig. 6). This is because nickel and aluminum were not

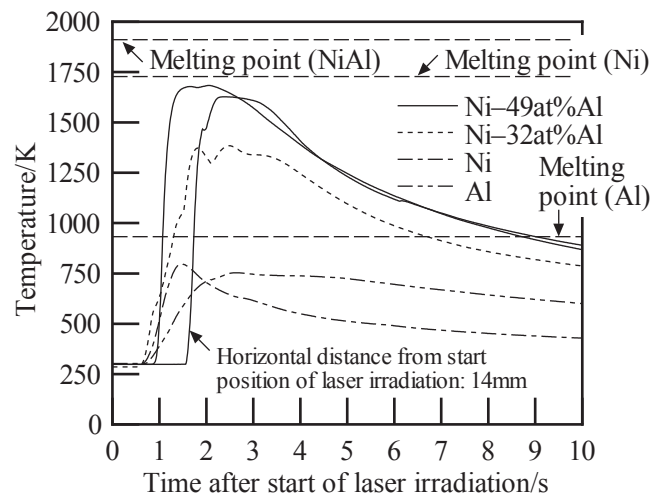


Fig. 9 Temperature changes in powders of nickel, aluminum and mixture during laser irradiation (measurement point: 2.5 mm in the -z direction from the surface of the powder mixture bed).

diffused sufficiently, and the composition range was kept at coexisting Ni_3Al and nickel (α) phases in Ni-Al binary phase diagram.¹⁵⁾

4. Discussions on Formation Mechanism

4.1 Temperature increase during laser irradiation

The temperature changes of the powders of nickel, aluminum and mixture during laser irradiation were measured by a R type thermocouple (platinum/13% rhodium-platinum). The thermocouple was inserted to 2.5 mm in the -z direction from the surface of the powder mixture bed from the start position of laser irradiation. The measurement results of the temperature of the powders during laser irradiation are shown in Fig. 9. Here the maximum temperature of the powder bed near the laser irradiation part is predicted to be locally much higher than the measured temperature from the consideration of the measurement position of the temperature. The temperature of the Ni-49at% Al powder mixture increased approximately 1680 K for 1.5 s, close to the melting point of nickel

(1728 K), while the temperature of the Ni–32 at% Al powder mixture increased approximately 1370 K. On the other hand, the temperatures of the unmixed powder of nickel or aluminum increased approximately 780 K and 750 K, respectively, and neither unmixed powders reached the melting point. The temperature increase rate of the Ni–49 at% Al powder mixture was faster than that of other powders. Furthermore, the temperature of the Ni–49 at% Al powder mixture increased approximately 1650 K for 1.5 s at the measurement point of 14 mm horizontally from the start position of laser irradiation.

These measurement results of the temperature agreed with the observation results of the laser-irradiated part as described in Section 3.1. Ignition of the Ni–49 at% Al powder mixture and no-ignition of the powders of the nickel, aluminum and Ni–32 at% Al mixture are indicated from the measurement results of the maximum temperature and the temperature increase rate indicate.

4.2 Enthalpy of formation for Ni–Al intermetallic compounds and ignition mechanism of powder mixtures

Concerning generation of reaction heat in transformation from liquid phase to solid phase of nickel, aluminum and Ni–Al intermetallic compounds are discussed from the relationship between enthalpy of formation and concentration of nickel in Al–Ni binary enthalpy diagram.^{21,22)} Since the change in enthalpy during phase transformation does not occur in nickel and aluminum, the reaction heat is not generated in their transformations. The reaction heat of 5–15 kJ/mol is generated in Ni–Al intermetallic compounds due to reduction in enthalpy (ΔH), and the reaction heat of NiAl ($|\Delta H| \approx 15 \text{ kJ/mol}^{21,22)$) is larger than that of Ni₃Al ($|\Delta H| \approx 5 \text{ kJ/mol}^{21,22)$). This implies the temperature increase of NiAl due to heat generation is larger than that of Ni₃Al in their transformations.

As described in Section 3.1, ignition of the powder mixture occurred in laser irradiation on the Ni–49 at% Al powder mixture, while ignition of the unmixed powder did not occur in laser irradiation on unmixed powder of nickel or aluminum. This indicates reaction heat is generated by the local formation of Ni–Al intermetallic compound near the melting interface between nickel and aluminum powders in laser irradiation on the powder mixtures. Due to reaction heat generated by laser irradiation on the powder mixtures, the temperature increase of the powder mixtures in laser irradiation is much larger than that of either nickel or aluminum unmixed powder as shown in Fig. 9.

On the other hand, ignition of the powder mixture did not occur in laser irradiation on the Ni–32 at% Al powder mixture. Since the powder mixture is heated above the melting point of aluminum by laser irradiation as shown in Fig. 9, NiAl is locally formed near the melting interface between nickel and aluminum powders. However, the reaction heat is difficult to be expanded from the interface to the surroundings because the amount of aluminum is insufficient surrounding the melting interface. As the results, the chain reaction does not occur, and the temperature increase of the Ni–32 at% Al powder mixture is smaller than that of the Ni–49 at% Al powder mixture. Thus Ni₃Al was

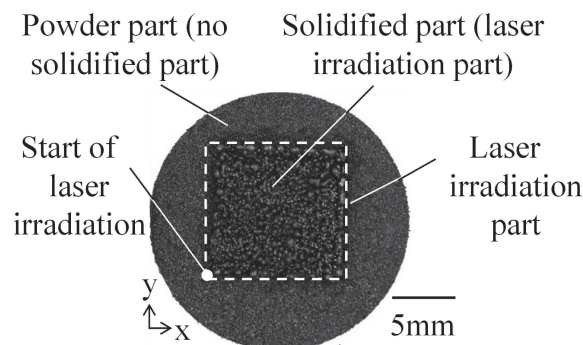


Fig. 10 Photograph of x-y surface of powder of NiAl intermetallic compound after laser irradiation (no ignition).

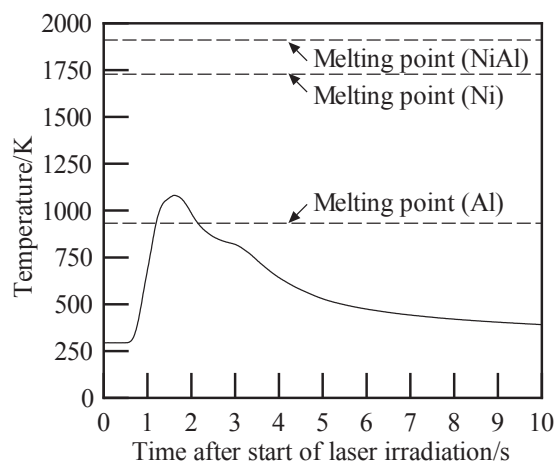


Fig. 11 Temperature change in NiAl intermetallic compound powder during laser irradiation.

formed only near the laser-irradiated part without ignition of the powder mixture.

Above formation mechanism of Ni–Al intermetallic compounds using laser irradiation is basically the same with the formation mechanism in the reaction synthesis using electric furnace heating.⁵⁾

4.3 Laser irradiation on NiAl intermetallic compound powder

To examine occurrence of the ignition, NiAl intermetallic compound powder was irradiated with laser with an average energy density of 150 J/mm^2 . The preparation of the powder was described in Section 2.1.

Figure 10 shows the OM photographs of the x-y surface of the NiAl intermetallic compound powder after laser irradiation. Ignition of the powder did not occur, and the powder was melted and solidified only near the surface of the laser-irradiated part. Figure 11 shows the measurement result of the temperature of the powder during laser irradiation. The temperature of the powder increased approximately 1080 K for 0.1 s just after start of laser irradiation. The temperature reached above the melting point of aluminum, however the temperature did not reach the melting point of nickel. This is because the reaction heat was not generated in the laser irradiation on the NiAl intermetallic compound powder.

From above results, it is concluded that ignition of Ni–49 at% Al powder mixture for formation of NiAl intermetal-

lic compound is due to the reaction heat between nickel and aluminum in laser irradiation on the powder mixtures.

5. Conclusions

In this study, NiAl intermetallic compound was formed by laser irradiation with an average energy density of 150 J/mm^2 on powder mixtures of nickel and aluminum. The solidified part was analyzed by microscopic observations, hardness measurement, EDX and XRD analyses. The formation mechanism was discussed. The following conclusions were obtained.

- (1) In laser irradiation on the Ni–49 at% Al powder mixture, NiAl intermetallic compound was formed by ignition of the powder mixture with maximum bulk volume of approximately $1.0 \times 10^4 \text{ mm}^3$ immediately after laser irradiation. The formation procedures of NiAl intermetallic compound were as follows. The reaction heat was generated on the interface of the nickel and aluminum powders by heating the powder mixture above the melting point of aluminum. Then chain reaction was expanded surrounding powder mixture by releasing the reaction heat. Finally, ignition of the powder mixture occurred.
- (2) In laser irradiation on the Ni–32 at% Al powder mixture, Ni_3Al intermetallic compound was formed only near the laser-irradiated part without igniting the powder mixture. This is because the generated reaction heat was insufficient amount to derive to the chain reaction for formation of NiAl or Ni_3Al . As the result, the ignition did not occur.
- (3) In laser irradiation on unmixed powder of nickel or aluminum, ignition of the powder did not occur, and the powder was melted and solidified only near the laser-irradiated part.

REFERENCES

- 1) N.S. Stoloff, C.T. Liu and S.C. Deevi: *Intermetallics* **8** (2000) 1313–1320.
- 2) C.T. Sims, N. Stoloff and W.C. Hagel: *Superalloys II*, (John Wiley & Sons, New York, 1987) p. 359.
- 3) K. Morsi: *J. Mater. Sci.* **47** (2012) 68–92.
- 4) D.E. Alman and N.S. Stoloff: *Int. J. Powder Metall.* **27** (1991) 29–41.
- 5) K. Morsi: *Mater. Sci. Eng. A* **299** (2001) 1–15.
- 6) A. Biswas, S.K. Roy, K.R. Gurumurthy, N. Prabhu and S. Banerjee: *Acta Mater.* **50** (2002) 757–773.
- 7) S.O. Moussa and K. Morsi: *Mater. Sci. Eng. A* **454–455** (2007) 641–647.
- 8) M. Kobashi and N. Kanetake: *Adv. Eng. Mater.* **4** (2002) 745–747.
- 9) H.X. Dong, Y. Jiang, Y.H. He, M. Song, J. Zou, N.P. Xu, B.Y. Huang, C.T. Liu and P.K. Liaw: *J. Alloy. Compd.* **484** (2009) 907–913.
- 10) H. Cui, L. Cao, Y. Chen and J. Wu: *J. Porous Mater.* **19** (2012) 415–422.
- 11) T. Shimizu: *Mater. Sci. Forum* **941** (2018) 1312–1317.
- 12) Z. Guo, P. Shen, J. Hu and H. Wang: *Opt. Laser Technol.* **37** (2005) 490–493.
- 13) Y. Yu, J. Zhou, J. Chen, H. Zhou, C. Guo, L. Wang and L. Yang: *Wear* **274–275** (2012) 298–305.
- 14) K.H. Hahn and K. Vedula: *Scr. Metall.* **23** (1989) 7–12.
- 15) T.B. Massalski, J.L. Murray, L.H. Bennett and H. Baker: *Binary Alloy Phase Diagrams*, (ASM International, Materials Park, OH, 1986) p. 140.
- 16) S. Kanatani, R. Matsumoto and H. Utsunomiya: *Key Eng. Mater.* **622–623** (2014) 861–867.
- 17) K. Nishiyama, Y. Yoshida, M. Mohri, N. Eguchi, S. Umekawa and S. Shite: *J. Japan Soc. Powder Powder Metall.* **38** (1991) 10–13.
- 18) S. Ochiai, I. Yamada and Y. Kojima: *J. Japan Inst. Metals* **54** (1990) 301–306.
- 19) A. Okada, Y. Yamamoto and R. Yoda: *Tetsu-to-Hagané* **73** (1987) 1186–1192.
- 20) *Structures and Properties of Aluminum*, (Japan Inst. Light Metals, 1991) p. 2.
- 21) A. Pasturel, P. Hicter, D. Mayou and F. Cyrot-Lackmann: *Scr. Metall.* **17** (1983) 841–846.
- 22) O. Kubachevski, C.B. Alcock and P.J. Spencer: *Materials Thermochemistry*, 6th Ed., (Pergamon Press, Oxford, 1993).